Supporting information for

A Facile Approach Using $MgCl_2$ to Formulating High Performance Mg^{2+} Electrolytes for Rechargeable Mg Batteries

Tianbiao Liu, Yuyan Shao, Guosheng Li*, Meng Gu, Jianzhi Hu, Suochang Xu, Zimin Nie, Xilin Chen, Chongmin Wang, Jun Liu**

Energy Process and Materials Division
Pacific Northwest National Laboratory (PNNL), *P.O. Box 999, Richland, WA 99352 (USA)*
E-mail: Tianbiao.Liu@pnnl.gov; Guosheng.Li@pnnl.gov; Jun.Liu@pnnl.gov

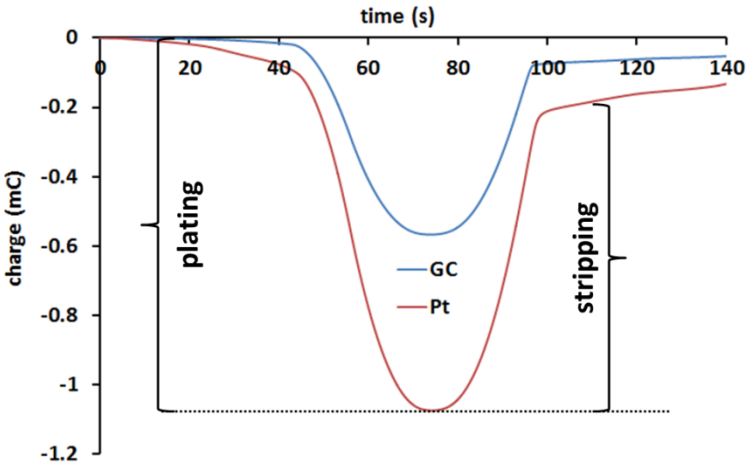

Figure S1. Plots of charge over time of the Mg plating and subsequent stripping processes of the $MgCl_2$-$AlCl_3$ electrolyte on GC (blue trace, 89% coulombic efficiency) and Pt (red trace, 90% coulombic efficiency) working electrodes. Conditions: scan rate, 50 mV/s; reference electrode, a Mg strip; counter electrode, glassy carbon; 22 °C; under 1.0 atm Ar.

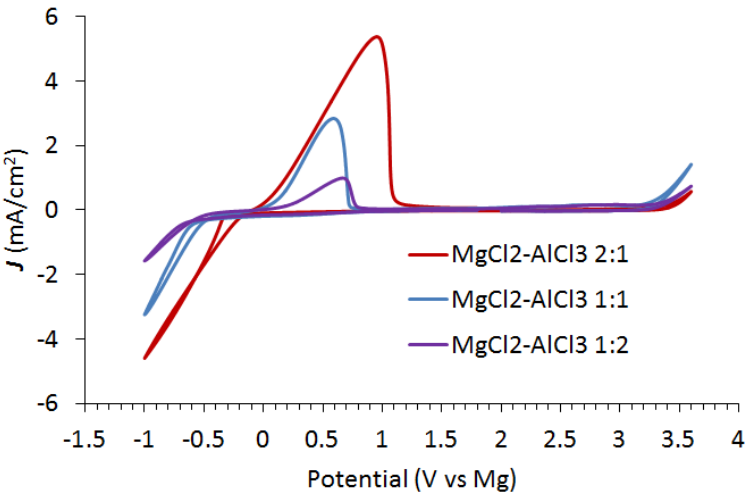

Figure S2. Comparison of CVs of the $MgCl_2$-$AlCl_3$ electrolyte at different ratios, 2:1 (red trace), 1:1 (blue trace) and 1:2 (purple trace) recorded on a GC electrode. Conditions: scan rate, 50 mV/s; reference electrode, a Mg strip; counter electrode, glassy carbon; 22 °C; under 1.0 atm Ar.

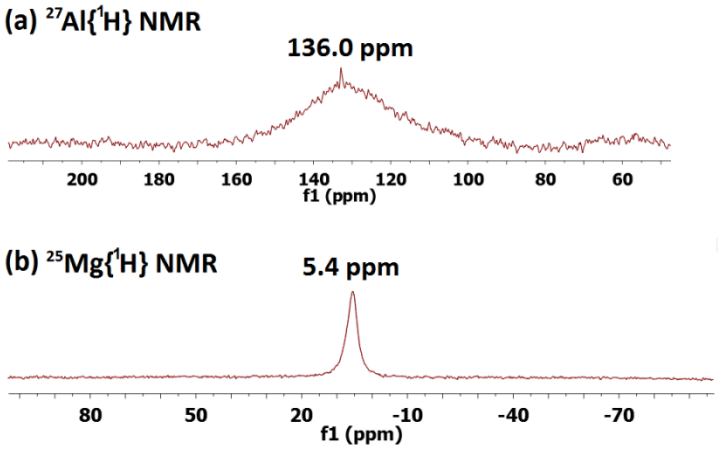

Figure S3. ^{27}Al{^{1}H} NMR and ^{25}Mg{^{1}H} NMR spectra of the $MgCl_2$-$AlPh_3$ electrolyte recorded in THF at 22 °C.

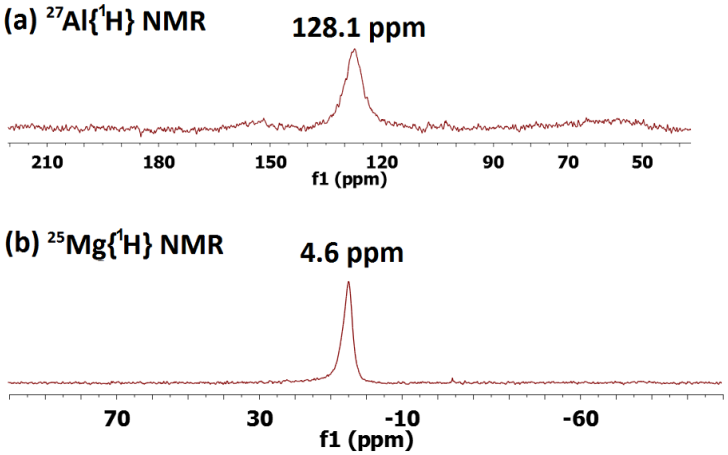

Figure S4. ^{27}Al{^{1}H} NMR and ^{25}Mg{^{1}H} NMR spectra of the $MgCl_2$-$AlEtCl_2$ electrolyte recorded in THF at 22 °C.

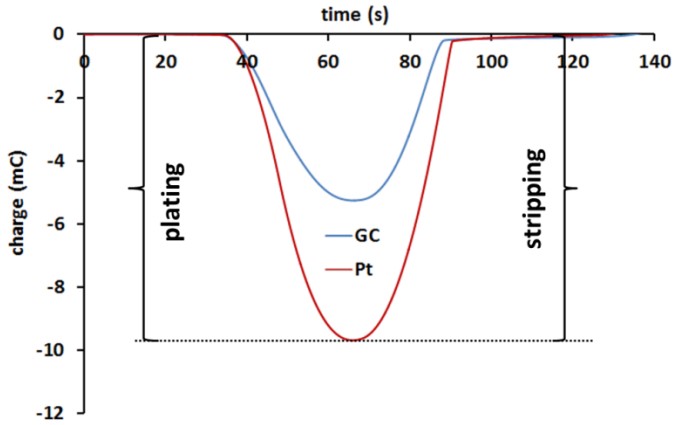

Figure S5. Plots of charge over time of the Mg plating and subsequent stripping processes of the $MgCl_2$-$AlPh_3$ electrolyte on GC (blue trace, ca. 100% coulombic efficiency) and Pt (red trace, ca. 100% coulombic efficiency) working electrodes. Conditions: scan rate, 50 mV/s; reference electrode, a Mg strip; counter electrode, glassy carbon; 22 °C; under 1.0 atm Ar.

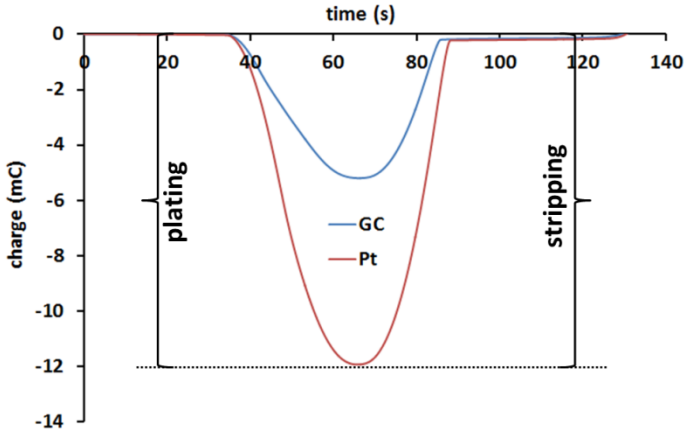

Figure S6. Plots of charge over time of the Mg plating and subsequent stripping processes of the $MgCl_2$-$AlEtCl_2$ electrolyte on GC (blue trace, ca. 100% coulombic efficiency) and Pt (red trace, ca. 100% coulombic efficiency) working electrodes. Conditions: scan rate, 50 mV/s; reference electrode, a Mg strip; counter electrode, glassy carbon; 22 °C; under 1.0 atm Ar.

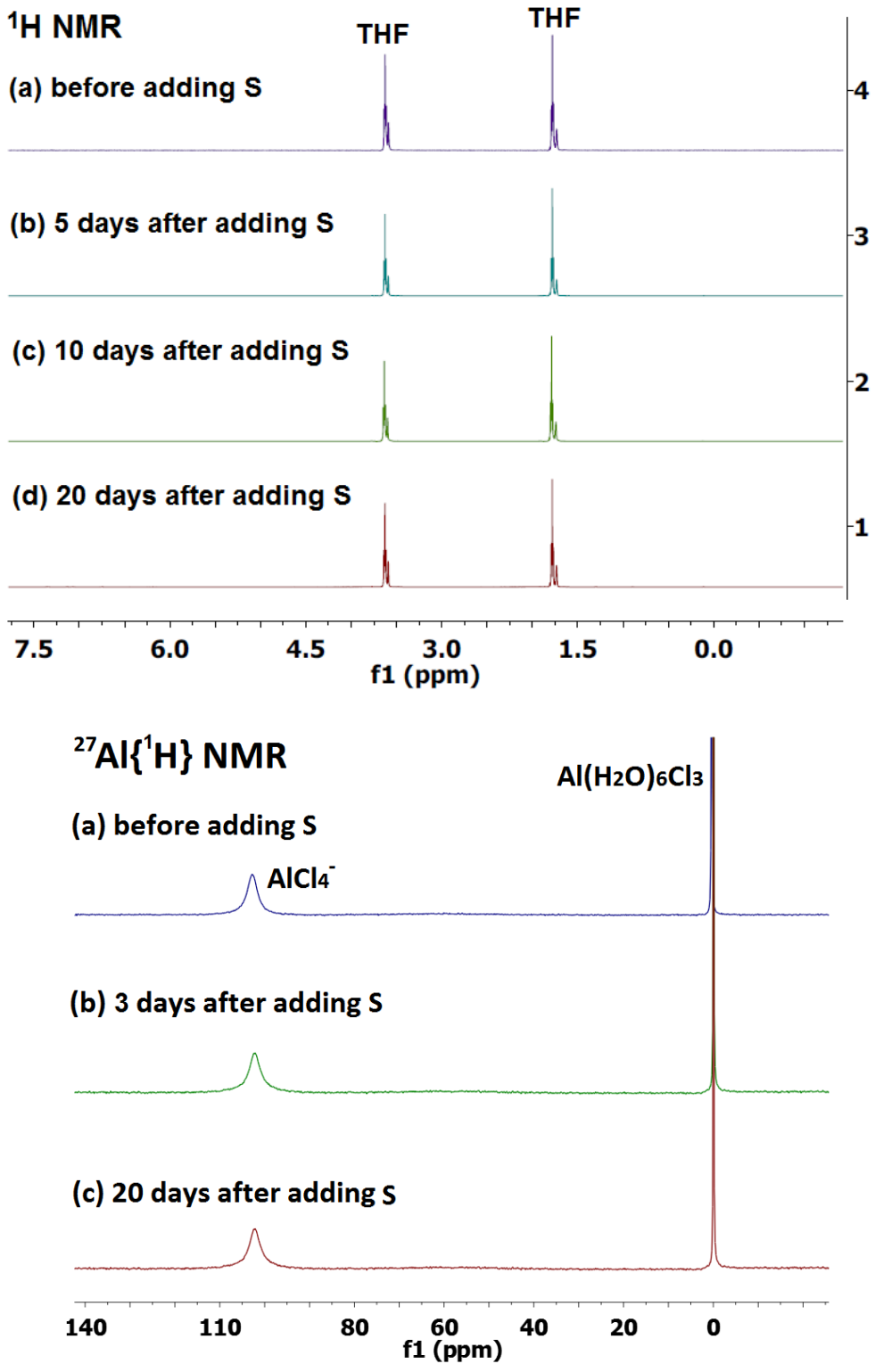

Figure S7. Sulfur compatibility of the $MgCl_2$-$AlCl_3$ electrolyte followed by ^{1}H NMR (top) and ^{27}Al{^{1}H} NMR (bottom) spectroscopy in THF at 22 °C. For ^{27}Al{^{1}H} NMR, a sealed

capillary containing 40 mM $Al(H_2O)_6Cl_3$ (0 ppm) as the internal reference for chemical shift and concentration was placed in the J-Young NMR tube.

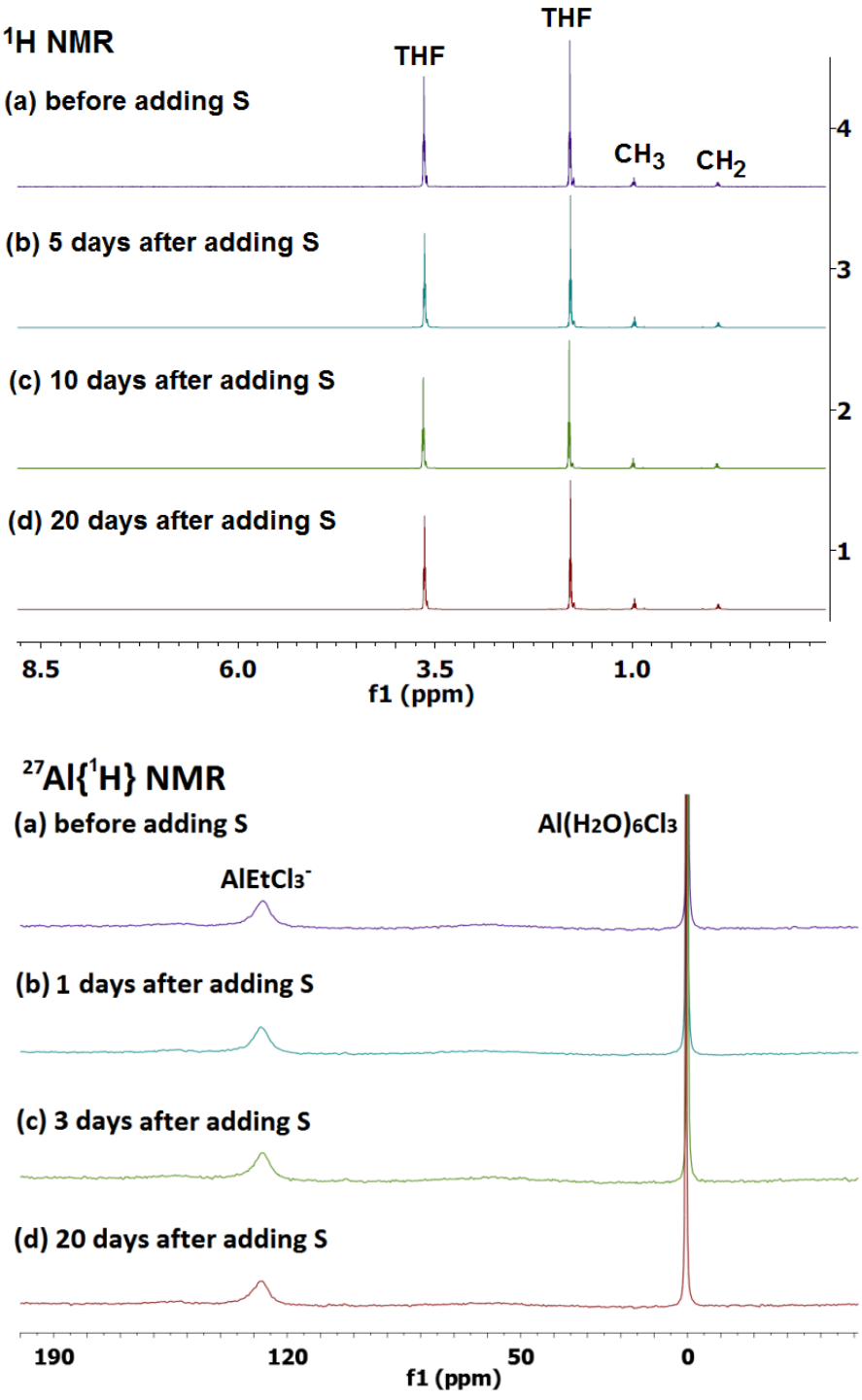

Figure S8. Sulfur compatibility of the $MgCl_2$-$AlEtCl_2$ electrolyte followed by ^{1}H NMR (top) and $^{27}Al\{^{1}H\}$ NMR (bottom) spectroscopy in THF at 22 °C. For $^{27}Al\{^{1}H\}$ NMR, a sealed capillary containing 40 mM $Al(H_2O)_6Cl_3$ (0 ppm) as the internal reference for chemical shift and concentration was placed in the J-Young NMR tube.

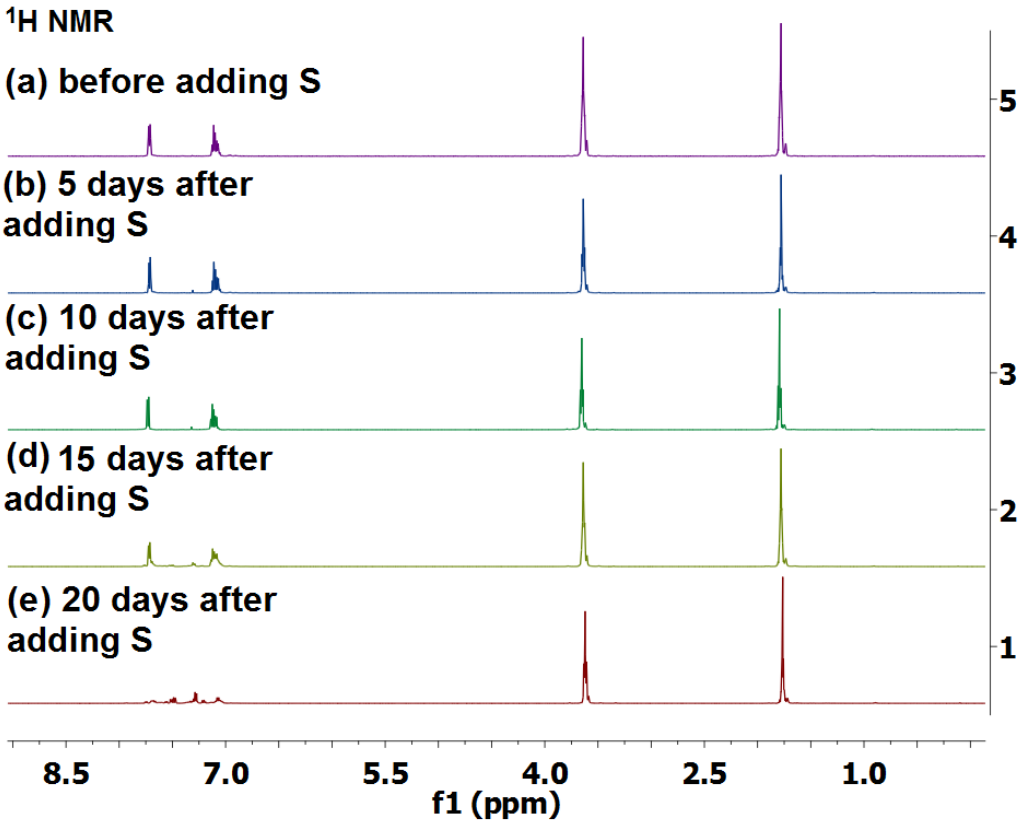

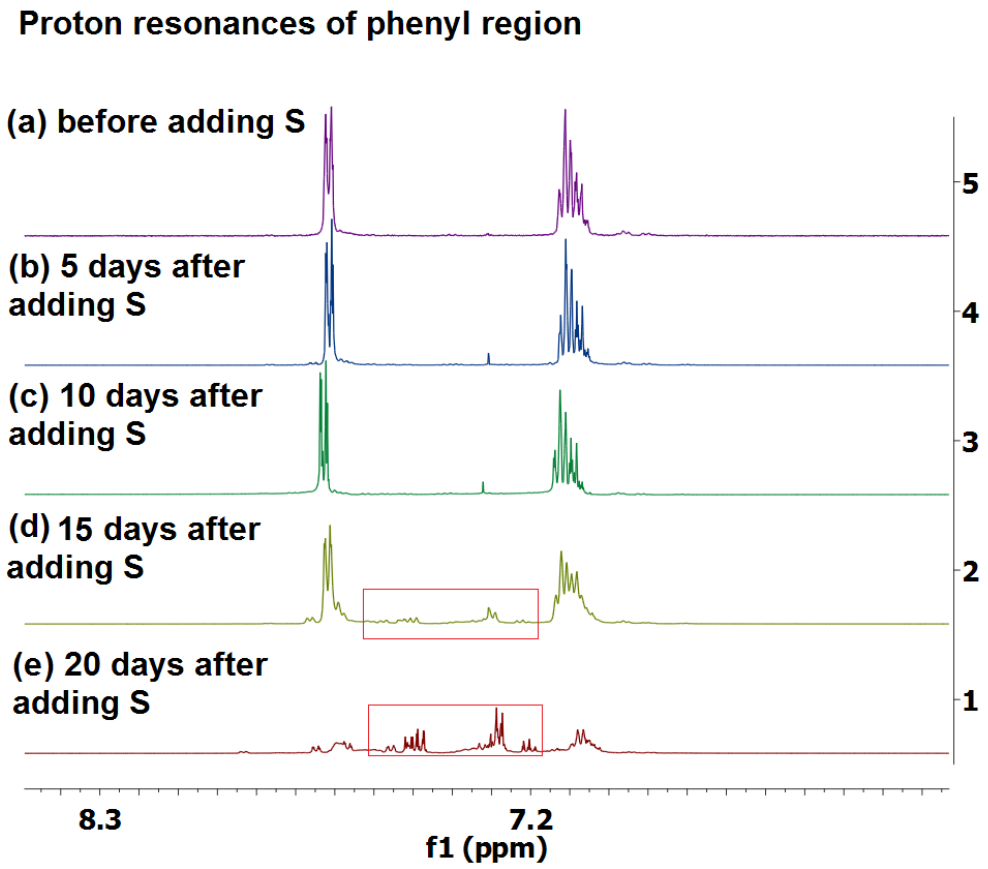

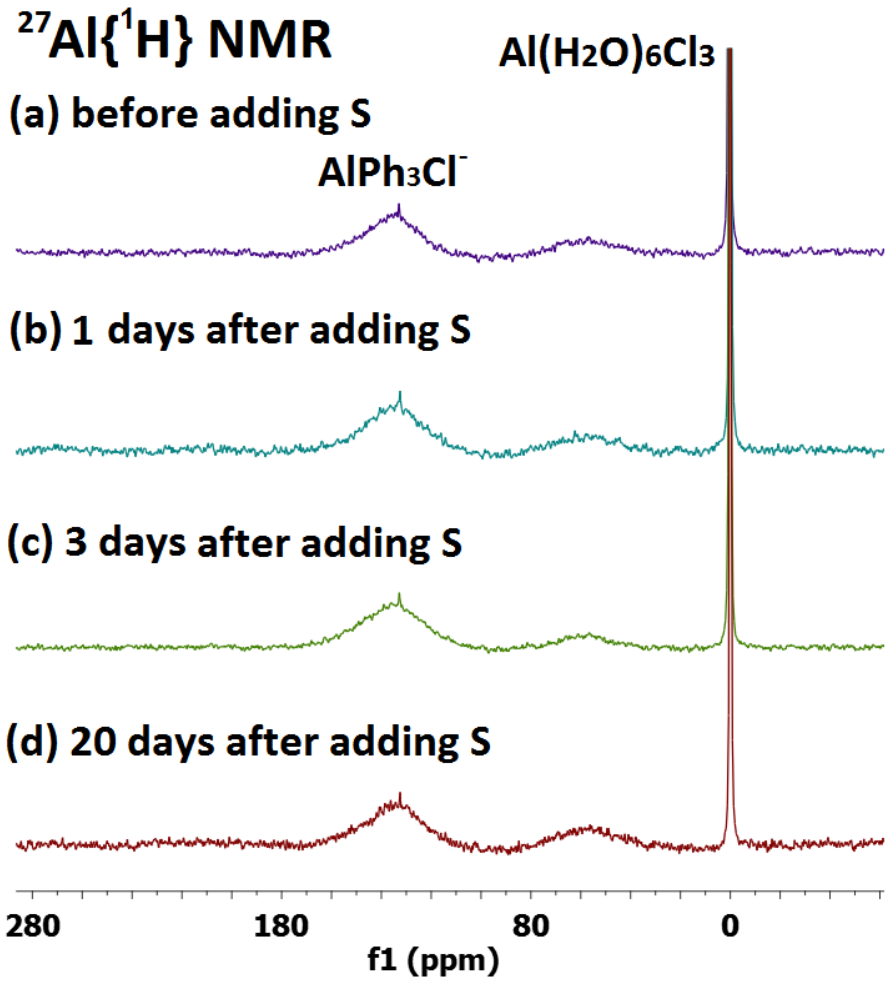

Figure S9. Sulfur compatibility of the $MgCl_2$-$AlPh_3$ electrolyte followed by ^1H NMR (top and middle) and $^{27}Al\{^1H\}$ NMR (bottom) spectroscopy in THF at 22 °C. In ^1H NMR spectra, the new peaks in red rectangles appear in the phenyl region and highlighted indicate degradation. For $^{27}Al\{^1H\}$ NMR, a sealed capillary containing 40 mM $Al(H_2O)_6Cl_3$ (0 ppm) as the internal reference for chemical shift and concentration was placed in the J-Young NMR tube.

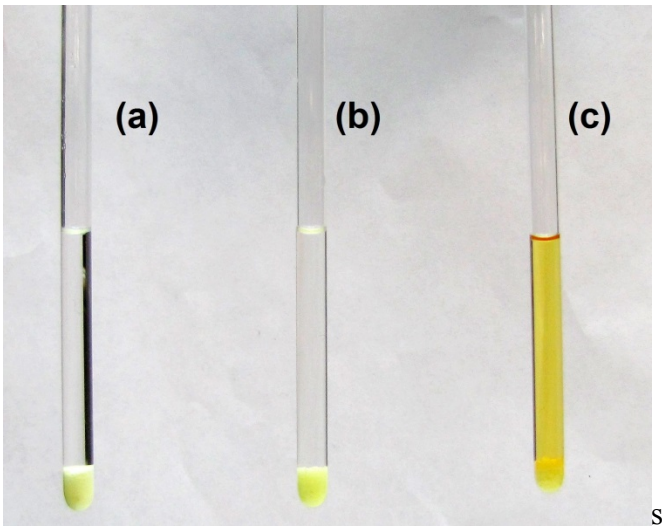

S

Figure S10. The images of the NMR tubes containing the $MgCl_2$-$AlCl_3$ electrolyte (a), the $MgCl_2$-$AlEtCl_2$ electrolyte (b), the $MgCl_2$-$AlPh_3$ electrolyte (c) after sulfur treatment for 20 days.

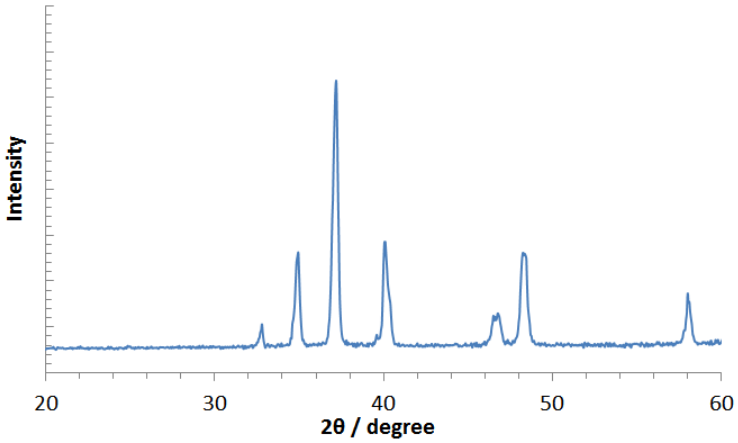

Figure S11. XRD pattern of deposited Mg on a Pt plate using the $MgCl_2$-$AlEtCl_2$ electrolyte.